Indian Journal of Science and Technology, *Vol 9(40), DOI: 10.17485/ijst/2016/v9i40/88878, October 2016*
ISSN (Print) : 0974-6846
ISSN (Online) : 0974-5645

Force Estimation of an Asymmetrical Pantograph for Different Damper Positions

Dumitru Cuciureanu[1], Costica Nituca[2*] and Gabriel Chiriac[2]

[1]"Q" SRL Iasi, Stradela Sf. Andrei nr.13, Iasi, Romania; office@qsrl.ro
[2]Technical University "Gheorghe Asachi" Iasi, Faculty of Electrical Engineering, Bd. D. Mangeron, nr. 21- 23, 700050 Iasi, Romania; gchiriac@tuiasi.ro, costica_nituca@yahoo.com

Abstract

Objectives: To estimate the optimal position of the damper (resort) for an asymmetrical pantograph drive system used for electric trains supply. **Methods/Analysis:** Different solutions to attach the damper are studied, considering the pull bar position, and the equations accordingly to every solution are estimated. The pantograph is droved by a resort, but it could be used any other mechanism, like pneumatic or hydraulic drive system. **Findings:** These analyses can be used to identify the optimal position of the pull bar from the main axle of the pantograph, in order to find the optimal work area of the pantograph, with small variation of the contact force and with a better contact between the pantograph and the contact line. **Novelty/Improvement:** An asymmetrical pantograph model at a scale of 1/4 is used for experiments, considering the force variation for lifting and descending of the pantograph. For the situations when the resort is attached by a crank (above or below of the oscillation point), in the relation of the force it appears a new expression.

Keywords: Contact Force, Damper Position Optimization, Pantograph, Resort

1. Introduction

Different pantographs are currently used in train vehicles around the world. With the exception of the Shinkansen 500 series telescopic pantograph, all high-speed railway pantographs are of the two-stage type[1]. The main characteristic of a pantograph is to assure a good current collecting, without interruptions of the current regardless of the height of the pantograph. For this, it is necessary for the pantograph to have a contact plan irrespective of the movement of the mechanical articulated system, a small inertia, a good lateral and transversal stability, to obtain in static and dynamic regime a contact pressure irrespective of the string height, and have a low sensibility at the aerodynamics effects. More of this, the pantograph needs to have a crosshead slipper with an adequate shape and way of suspension for the contact characteristics. Its shape, size and fixation depend on the characteristics of the electric current, on the geometrical characteristics of the contact line[2] especially on the catenary irregularities which may cause serious fluctuation of contact force, even leading to the pantograph coming off the catenary[3].

In the general nonlinear model, the pantograph model is represented in terms of the following kinematic linkages: a lower frame arm, an upper frame arm and a head link. The entire mechanism is raised by a torque applied to a link of the arm. A frame suspension model provides an uplift force to the pantograph. The input force is assured by a suspension, usually a resort or pneumatic system (actuator) which acts horizontally, applying a torque to the lower arm. This input force may vary in time and has to overcome the weight of the mechanism but also must provide the uplift force against the wire[4]. In some cases there are used only dampers (resorts) to assure the uplift force, as for the pantograph for the Korean high speed train[5]. The model of the pantograph can be realized with two masses[6] with accent on the active control of the pantograph but also a model in three dimensions with the advantages to consider many hypothesizes[7].

Low contact forces may lead to loss of contact,

** Author for correspondence*

resulting in electric arcing and power interruptions. On the other hand, too large contact forces may cause rapid wear of the carbon skates. Moreover, the pantograph may exhibit unexpected motions even when the contact-force variation is kept within a reasonable range. Thus, vertical dynamics of the carbon-strip suspension is also studied with an aim of improving the reliability and safety of running trains[8]. The variation on the head suspension resort stiffness reflects factors related to operation conditions, maintenance and material degradation. The variation on the lower damper of the pantograph represents factors related to usage in service, degradation and lack of maintenance[9].

The pneumatic actuator is working typically at 3.5-4.5 barr and in order to obtain a constant transmission ratio from air pressure to static force between sliding surfaces, the geometry of coupling between the actuator and pantograph is optimized[10]. To improve the dynamical response of the pantograph are used different solutions according to the position of the active suspension stage of the pantograph: a) active suspension system between sliding bows and mobile frame and b) active actuator on the mobile frame, with a passive suspension system placed under sliding bows. The layout *b* is preferred usually because their shape has less effect on the aerodynamic behavior of the pantograph[10], has lesser limitation concerning shape, weight and is better protected from the harsh environmental conditions.

There are also studies regarding unconventional methods to supply the electric traction vehicles[11]. All these studies have to be considered having into attention the environmental friendly aspects of the different types of transportation systems, considering the large efforts to improve the quality of the emissions and to reduce the pollution over the medium[12].

With these considerations it is useful to study the resort/damper position according to the frame of the pantograph, in order to estimate the pantograph dynamics and forces.

2. Estimation of the Lifting Force of the Pantograph

First it is to estimate the vertical force F developed due to the resort R of the pantograph over the contact line CL depending on the high of the pantograph. To simplify, the pantograph is considered as a bar T with the weight *G*, length *l*, and jointed in the point O (Figure 1). In the point O_2 the bar is linked to the upper arm of the pantograph (Figure 2). The resort *R* with a length of l_R = a + (b + x) + c drives the bar, where *x* is a variable. It is considered that there is no friction into the joints of the pantograph. The pantograph will have a vertical motion v_v. (Figure 1)

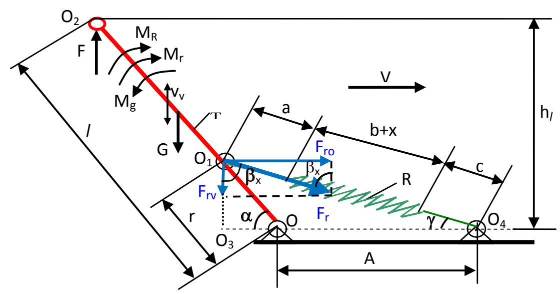

Figure 1. Kinematics of the asymmetrical pantograph.

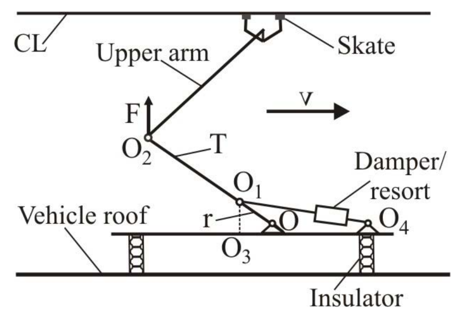

Figure 2. Simplified physical representation of the asymmetrical pantograph.

The torque due to the force G related to the point O is:

$$M_g = G\frac{l}{2}\cos\alpha \tag{1}$$

The torque M_r related to the point O due to the resort can be estimated starting from the force F_r given by the resort, composed from horizontal and vertical components, $\overline{F}_r = \overline{F}_{ro} + \overline{F}_{rv}$:

$$M_r = F_{ro} r \sin\alpha - F_{rv} r\cos\alpha \tag{2}$$

where $OO_1 = r$.

Considering $F_{ro} = F_r \sin\beta_x$ and $F_{rv} = F_r \cos\beta_x$ and replacing into the equation (2) it results:

$$\begin{aligned} M_r &= F_r r \sin\beta_x r\sin\alpha - F_r \cos\beta_x r\cos\alpha \\ &= F_r r\left(\sin\beta_x \sin\alpha - \cos\beta_x \cos\alpha\right) \end{aligned} \tag{3}$$

But $\cos\beta_x = \frac{r\sin\alpha}{k_1 + x}$ and $\sin\beta_x$

$$= \sqrt{1 - \frac{r^2\sin^2\alpha}{(k_1+x)^2}} \text{ with } k_1 = a + b + c$$

Replacing into equation (3):

$$M_r = F_r r\left[\sin\alpha\sqrt{1-\frac{r^2\sin^2\alpha}{(k_1+x)^2}}-\frac{r\sin\alpha}{k_1+x}\cos\alpha\right] \quad (4)$$

and

$$M_r = F_r r\sin\alpha\frac{1}{(k_1+x)}\left[\sqrt{(k_1+x)^2-r^2\sin^2\alpha}-r\cos\alpha\right] \quad (5)$$

In the triangle $O_1O_3O_4$

$$(k_1+x)^2 = r^2\sin^2\alpha+(r\cos\alpha+A)^2 \quad (6)$$

and

$$x=\sqrt{r^2\sin^2\alpha+r^2\cos^2\alpha+2Ar\cos\alpha+A^2}-k_1, \quad (7)$$

or

$$x=\sqrt{A^2+r^2+2Ar\cos\alpha}-k_1. \quad (8)$$

Replacing the value (k_1+x) into (5) it results the intermediate relation:

$$M_r = F_r r\sin\alpha\frac{1}{k_0+x}\left[\sqrt{r^2\sin^2\alpha+(r\cos\alpha+A)^2-r^2\sin^2\alpha}-r\cos\alpha\right]$$

Finally:

$$M_r=\frac{F_r rA\sin\alpha}{k_0+x} \quad (9)$$

The force of the resort is given by a relation as:

$$F_r = k_0 x \quad (10)$$

where k_0 is a constant of the resort and x is the elongation of the resort. Thus:

$$M_r=\frac{F_r rA\sin\alpha}{k_1+x}=\frac{k_0 xAr\sin\alpha}{k_1+x} \quad (11)$$

Replacing the value of x in (8):

$$M_r=\frac{k_0 Ar\sin\alpha\left(\sqrt{A^2+r^2+2Ar\cos\alpha}-k_1\right)}{\left(k_1+\sqrt{A^2+r^2+2Ar\cos\alpha}-k_1\right)} =\frac{k_0 Ar\sin\alpha\left(\sqrt{A^2+r^2+2Ar\cos\alpha}-k_1\right)}{\sqrt{A^2+r^2+2Ar\cos\alpha}} \quad (12)$$

Considering by notation $A^2+r^2=m$ and $2rA=n$ it results:

$$M_r=\frac{k_0 Ar\sin\alpha\left(\sqrt{m+n\cos\alpha}-k_1\right)}{\sqrt{m+n\cos\alpha}} =k_0 Ar\sin\alpha\left(1-\frac{k_1}{\sqrt{m+n\cos\alpha}}\right) \quad (13)$$

Summing the torques M_r and M_g:

$$M_R = M_r + M_g = k_0 Ar\sin\alpha \left(1-\frac{k_1}{\sqrt{m+n\cos\alpha}}\right)-G\frac{l}{2}\cos\alpha \quad (14)$$

The force due to the torque M_R into the point O_3 (Figure 3):

$$F=\frac{M_R}{l\cos\alpha}=\frac{k_0 Ar\sin\alpha}{l\cos\alpha}\left(1-\frac{k_1}{\sqrt{m+n\cos\alpha}}\right)-\frac{G}{2} \quad (15)$$

Replacing $\frac{k_0 Ar}{l}$ with k_2 it results:

$$F=k_2\sin\alpha\frac{1}{\cos\alpha}\left[1-\frac{k_1}{\sqrt{m+n\cos\alpha}}\right]-\frac{G}{2} \quad (16)$$

or

$$F=k_2 tg\alpha\left[1-\frac{k_1}{\sqrt{m+n\cos\alpha}}\right]-\frac{G}{2} \quad (17)$$

3. Resort Position for the Pantograph Drive System

The equation (17) shows the link between the force F of the pantograph acting on the contact line and the angle α, and the link between the force F and the height of the pantograph skate h_l because of the relation:

$$h_l = l\sin\alpha \quad (18)$$

The equation (17) has three elements:

$$1.)\ k_2 tg\alpha;\quad 2.)\ \frac{k_1k_2 tg\alpha}{\sqrt{m+n\cos\alpha}};\quad 3.)\ \frac{G}{2}. \quad (19)$$

where:

$$m=A^2+r^2 n=2Ar; k_2=\frac{k_0 Ar}{l}; k_3 =A-(a+b); k_4=\frac{k_0 rk_3}{l}; k_5=\frac{k_0 r^2}{l} \quad (20)$$

For a variation of the angle α = 0…90^0, the first and the second expressions vary in different ways, that is the vertical force F is not constant and depend on the high of the skate. Thus, it is not possible to have a perfect constant force by using a resort.

Thus, it is important to know which the best options to obtain a constant force are. In this situation, it is important to analyze the modalities to attach the resort on the bar of the pantograph related to a fixed point.

4. Possibilities for the Resort Drive System Attachment

In this chapter there are presented some solutions for the resort position which is attached between the pantograph bar and a fixed point. There are also presented the equations accordingly to every solution. The pantograph is considered as a simplified system with a bar supported by the roof of the locomotive and used to collect energy from the contact line. With the above conditions, it results different situations to attach the resort and the bar and we consider for the analysis 12 cases.

In the first case, in extension of the bar T, in the point O_1, there is a pull bar on length *r*. One of the resort ends is jointed in the point O_1, and the other end is fixed in the point O_4, at the distance A, in the same plane with the inferior arm *r*, which is, in the same time, the support and the joint point O of the bar of the pantograph. Considering the movement direction of the train (the direction of the speed of the vehicle *V*), we consider that the resort is placed "in front" of the pantograph.

In the second case, the pull bar r is in the same position as the in the first case, but the support and the joint point of the pantograph bar is the point O_1, in the extension of the bar T with the bar *r*. The resort is "behind" the pantograph.

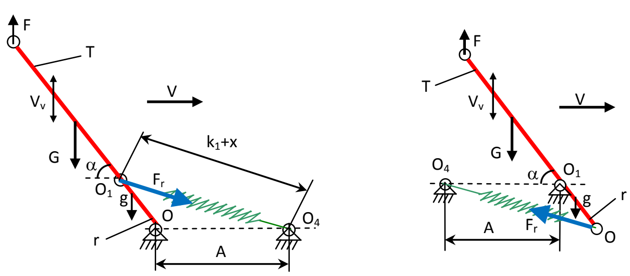

Figure 3. (a) 1st case: the resort is placed "in front" of the pantograph, (b) 2nd case: the resort is placed "behind" of the pantograph.

Considering the Figures 3(a) and 3(b):

$$1^{st}\text{ case: } F = k_2 tg\alpha - \frac{k_1 k_2}{\sqrt{m + n\cos\alpha}} tg\alpha - \frac{G}{2} \quad (21)$$

$$2^{nd}\text{ case: } F = k_2 tg\alpha - \frac{k_1 k_2}{\sqrt{m + n\cos\alpha}} tg\alpha - \frac{1}{2}\left(G - g\frac{r}{l}\right) \quad (22)$$

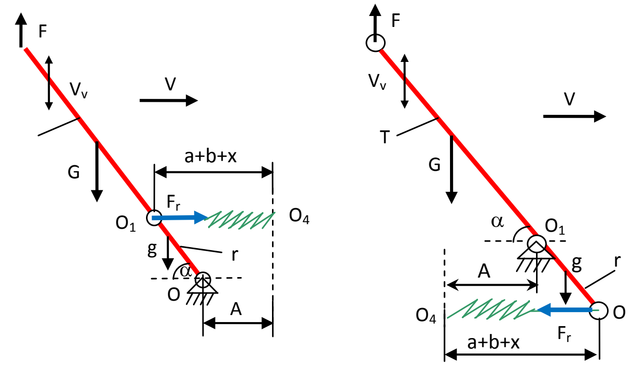

Figure 4. (a) 3rd case: the resort is horizontal and "in front" of the pantograph. (b) 4th case: the resort is horizontal and "behind" of the pantograph.

In the 3rd case the pull bar r is in the same position as in the first case, but the resort is jointed in horizontal plane "in front" of the pantograph. One of its ends is on the point O_1 and the other in the point O_4, at the distance *A*. In the 4th case the pull bar r is as in the second case, but the resort is horizontal and "behind" the pantograph, at the distance A from the support in O_1. Considering the Figures 4(a) and 4(b):

$$3^{rd}\text{ case: } F = k_4 tg\alpha + k_5 \sin\alpha - \frac{G}{2} \quad (23)$$

$$4^{th}\text{ case: } F = k_4 tg\alpha + k_5 \sin\alpha - \frac{1}{2}\left(G - g\frac{r}{l}\right) \quad (24)$$

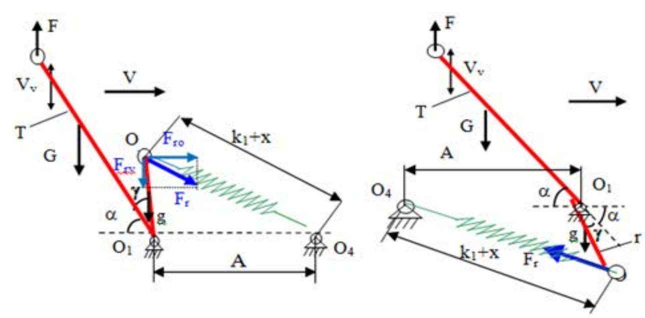

Figure 5. (a) 5th case: the pull bar r is "in front" and above of the pantograph, at an angle γ, (b) 6th case: the pull bar r is "in front" and below of the pantograph, at an angle γ.

In case 5 the pull bar *r* is rigid fixed on the inferior part of the bar T, in the point O_1 (a joint point for the bar T) "in front" of the pantograph at an angle γ (which is considered as constant) from the normal position of the pantograph (Figure 5(a)). At the other end of the bar *r*, in point O, is fixed an end of the resort *R*. The other end of the resort is fixed in point O_4.

In case 6 (Figure 5(b)) the pull bar *r* is in extension of the bar T, but at the angle γ. The resort has an end in the point O and the other in O_4, in the same plane with the point O_1.

5[th]case $$F = k_2 \frac{\sin(\alpha+\gamma)}{\cos\alpha} - \frac{k_1 k_2}{\sqrt{m + n\cos\alpha}} \frac{\sin(\alpha+\gamma)}{\cos\alpha} - \frac{1}{2}G - \frac{g}{2}\frac{r}{l}\frac{\cos(\alpha+\gamma)}{\cos\alpha} \quad (25)$$

6[th] case: $$F = k_2 \frac{\sin(\alpha+\gamma)}{\cos\alpha} - \frac{k_1 k_2}{\sqrt{m + n\cos\alpha}} \frac{\sin(\alpha+\gamma)}{\cos\alpha} - \frac{1}{2}G + \frac{g}{2}\frac{r}{l}\frac{\cos(\alpha+\gamma)}{\cos\alpha} \quad (26)$$

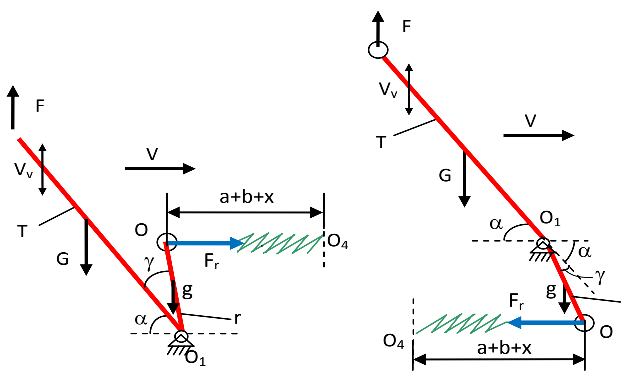

Figure 6. (a) 7[th] case: the pull bar is "in front" of the pantograph, at an angle γ, with horizontal resort, (b) 8[th] case: the pull bar is "behind" of the pantograph, at an angle γ, with horizontal resort.

In case 7 (Figure 6(a)) the bar *r* is as in the case 5, but the resort is horizontally placed "in front" of the pantograph between the point O and O_4, at a distance a + b + x.

In case 8 (Figure 6(b)) the bar *r* is as in the case 6, but the resort is horizontally placed "below" the pantograph, between the point O and O_4, at a distance a + b + x.

7[th] case $$F = k_4 \frac{\sin(\alpha+\gamma)}{\cos\alpha} + k_5 \frac{\sin(\alpha+\gamma)}{\cos\alpha} \cos(\alpha+\gamma) - \frac{1}{2}G - g\frac{r}{2l}\frac{\cos(\alpha+\gamma)}{\cos\alpha} \quad (27)$$

8th case $$F = k_4 \frac{\sin(\alpha+\gamma)}{\cos\alpha} + k_5 \frac{\cos(\alpha+\gamma)}{\cos\alpha} \sin(\alpha+\gamma) - \frac{1}{2}G + \frac{1}{2}\frac{gr}{l}\frac{\cos(\alpha+\gamma)}{\cos\alpha} \quad (28)$$

In case 9 the bar *r* is fixed in the point O_1, "behind" the pantograph and at the angle g from the normal position of the pantograph, as seen in Figure 7(a). In the point O is fixed one of the ends of the resort and the other is fixed in point O_4, "in front" of the pantograph, at distance A.

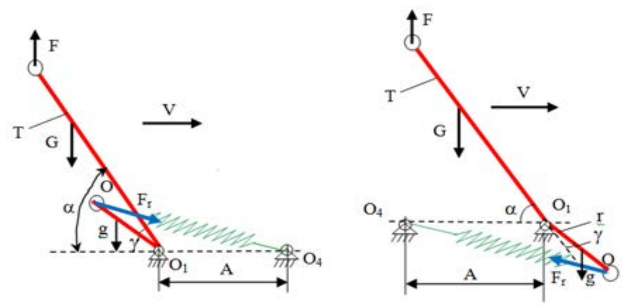

Figure 7. (a) 9[th] case: the pull bar is "behind" and above of the pantograph point O1, at an angle γ, (b) 10[th] case: the pull bar is "in front" and below of the pantograph point O1, at an angle γ

In case 10 (Figure 7(b)) the bar *r* is place in extension of the bar T "in front" of the pantograph at the angle g. The resort is fixed between the points O, below the pantograph, and the point O_4, in the same horizontal with the point O_1.

case 9: $$F = k_2 \frac{\sin(\alpha-\gamma)}{\cos\alpha} - \frac{k_1 k_2}{\sqrt{m + n\cos(\alpha-\gamma)}} \frac{\sin(\alpha-\gamma)}{\cos\alpha} - \frac{1}{2}\left[G + g\frac{r}{l}\frac{\cos(\alpha-\gamma)}{\cos\alpha}\right] \quad (29)$$

case:10. $$F = k_2 \frac{\sin(\alpha-\gamma)}{\cos\alpha} - \frac{k_1 k_2}{\sqrt{m + n\cos(\alpha-\gamma)}} \frac{\sin(\alpha-\gamma)}{\cos\alpha} - \frac{1}{2}\left[G - g\frac{r}{l}\frac{\cos(\alpha-\gamma)}{\cos\alpha}\right] \quad (30)$$

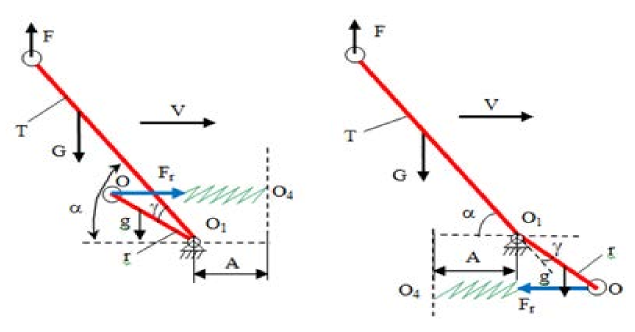

Figure 8. (a) 11th case: the pull bar is "behind" of the pantograph, at angle γ, with horizontal resort, (b) 12th case: the pull bar is "in front" of the pantograph, at angle γ with horizontal resort.

In case 11 (Figure 8(a)), the bar is placed as in the case 9, and the resort is placed horizontally “in front” of the pantograph. In case 12 (Figure 8(b)) the bar is placed as in the case 10 and the resort is placed horizontally “below” the pantograph.

$$\text{case:11}\quad F=k_4\frac{\sin(\alpha-\gamma)}{\cos\alpha}+k_5\frac{\sin(\alpha-\gamma)}{\cos\alpha}\cos(\alpha-\gamma)-\frac{1}{2}G-\frac{g}{2}\frac{r}{l}\frac{\cos(\alpha-\gamma)}{\cos\alpha} \tag{31}$$

$$\text{Case:12}\quad F=k_4\frac{\sin(\alpha-\gamma)}{\cos\alpha}+k_5\frac{\sin(\alpha-\gamma)}{\cos\alpha}\cos(\alpha-\gamma)-\frac{1}{2}G+\frac{g}{2}\frac{r}{l}\frac{\cos(\alpha-\gamma)}{\cos\alpha} \tag{32}$$

5. Simulations and Results

For the simulations there are considered the data[13]: l=0.510

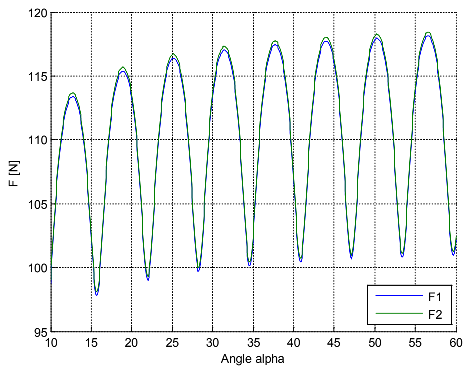

(a) 1st and 2nd cases.

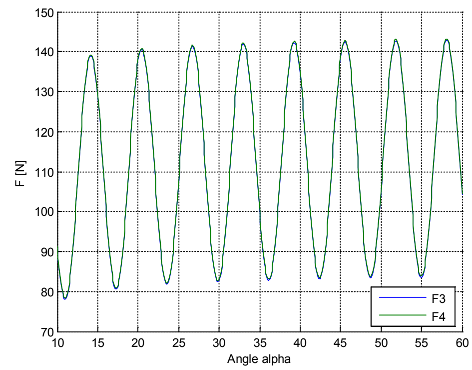

(b) 3rd and 4th cases.

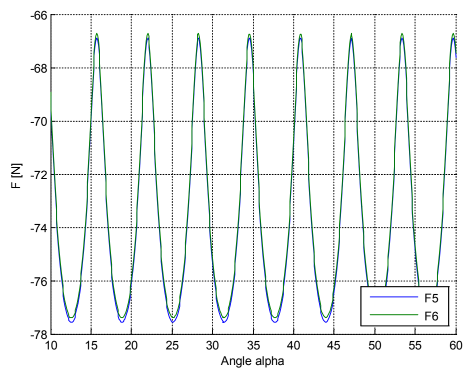

(c) 5th and 6th cases.

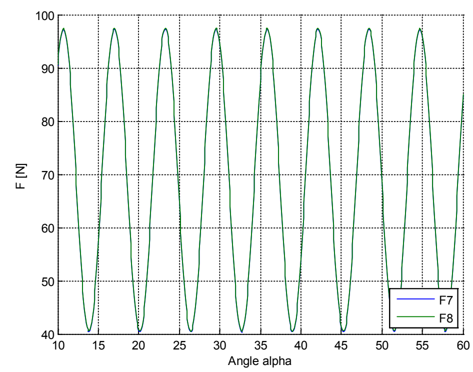

(d) 7th and 8th cases.

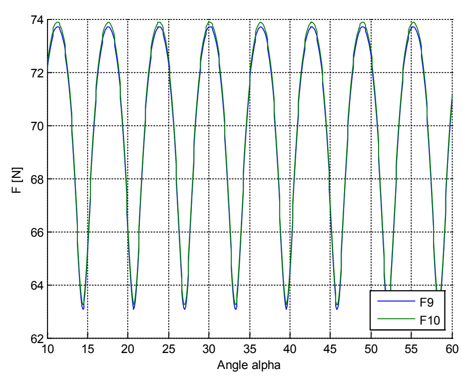

(e) 9th and 10th cases.

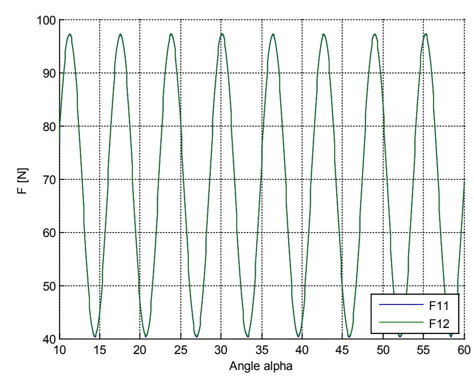

(f) 11th and 12th cases.

Figure 9. Simulations for the vertical force in cases 1-12.

Table 1. Contact force values

	F_1 [N]	F_2 [N]	F_3 [N]	F_4 [N]	F_5 [N]	F_6 [N]	F_7 [N]	F_8 [N]	F_9 [N]	F_{10} [N]	F_{11} [N]	F_{12} [N]
Minimum values	97.8	98.09	78.11	78.4	-77.57	-77.4	40.35	40.52	63.06	63.23	40.28	40.45
Maximum values	118.1	118.4	142.9	143.2	-66.89	-66.7	97.27	97.44	73.72	73.89	97.28	97.29
Force variation	20.3	20.31	64.79	64.8	-10.68	-10.7	56.92	56.92	10.66	10.66	57.0	56.84

m; G=5.550 kg; a=0.01 m; b=0.255 m; c=0.01 m; x=0.225 m; α=600; γ=50; r=0.55 m; A=1.650 m; k_0=50Ns/m; g=0.550 kg. The results of the simulations are presented in Figure 9 and Table 1.

The pantograph has a movement close to a sinusoid. To avoid large amplitudes and the detachments from the contact wire, the pantograph has to assure the maximum and minimum amplitude of the sinusoid. These values depend on the position of the pull bar and of the resort drive system. Analyzing the simulations in Figure 9 and the values in table 1, we can conclude:

a. The forces have positive values, except the case 5 and the case 6

b. There are three groups according to the variation of the force:

- Large variation of the force, with the cases 3rd (64.79N), 4th (64.8N), 7th (56.92N), 8th (56.92N), 11th (57N) and 12th (56.84N); these cases cannot be considered because the variation of the force is to large, which gives a delayed reaction time for the pantograph in order to follow the trajectory of the contact wire;
- Medium variation of the force, with the cases 1st (20.3N) and 2nd (20.31N). These cases could be considered for the pantograph system drive, because the reaction time is lower and the skate of the pantograph can easily follow the trajectory of the contact wire; and
- Small variation of the force, with the cases 9th (10.66N), 10th (10.66N), 5th (-10.68N) and 6th (-10.7N). In these situations there are two cases with positive values and two with negative values. In practice, this can be realized by replacing the expansion resort with a compression one, with the same mechanical parameters. In these cases the reaction times are low assuring a good contact between the skate and the contact wire. These solutions are to be recommended for the pantograph drive system.

c. The medium value for the maximum forces considering all the twelve cases is 99.42 N, while the medium value for the minimum forces is 66.27 N.

6. Test bench Experiments

A practical analysis is made considering the force variation on lifting and descending of the pantograph. From the 12 cases presented above we consider two cases, the 4th case and the 9th case, because they have the resort horizontal and "behind" the pantograph, at the distance A from the support in O1 (case 4), and the bar r is fixed "behind" the pantograph and at the angle γ from the normal position of the pantograph, but in the point O is fixed one of the ends of the resort and the other is fixed in point O4, "in front" of the pantograph, at distance A (case 9).

For these two extreme situations there are determined the static characteristic F =f(α) of the pantograph for lifting and descending, considering a bench stand as in Figure 10. An asymmetrical pantograph (1) at a scale of ¼ as regarding a real system. The pantograph has two graphite skates (2) and the classical mechanical lifting (resort) system (3) used for the main lifting force. The pull bar *r* could be placed in different positions, (4) and (5), "in front" and "behind" of the pantograph in order to analyze the considered positions.

The pantograph model has a low inertia, a good lateral stability, a constant contact pressure for a specific high and a low wear of the graphite skate.

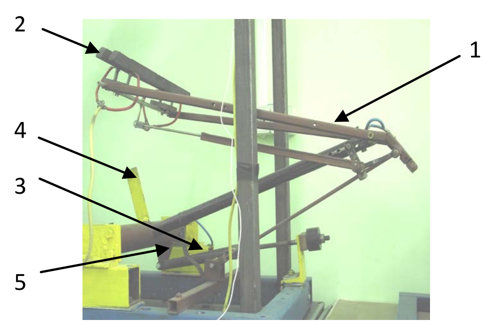

Figure 10. The asymmetrical pantograph used for the experimental tests.

Figure 11 presents the static characteristics F =f(α) for the 4th case. The experimental characteristic has a maximum of 145 N for lifting and 144 N for descending, while the minimum values are 76 N for lifting and 74 N for descending. It is to observe the difference of 2 N between the lifting force and descending force. Comparing with the simulations for the 4th case, the difference is about 1.8 N for the maximum force and 4.4 N for the minimum force.

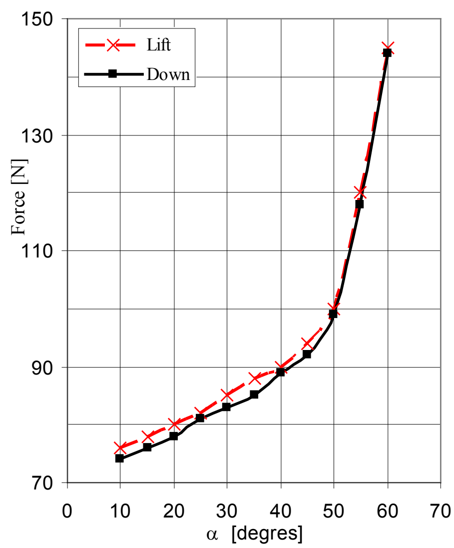

Figure 11. The static characteristic F =f(α) for the 4th case.

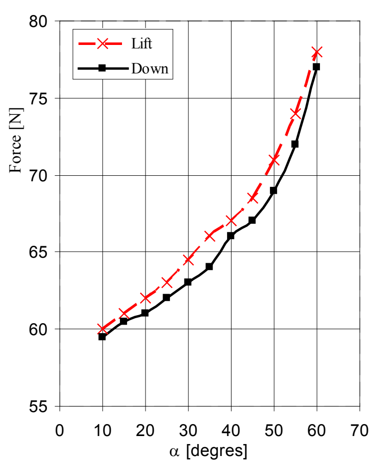

Figure 12. The static characteristic F =f(α) for the 9th case.

Figure 12 presents the static characteristics F =f(α) for the 9th case. The experimental characteristic has a maximum of 78 N for lifting and 77 N for descending, while the minimum values are 60 N for lifting and 59.5 N for descending. The difference between the lifting force and descending force is maximum 1N. Comparing with the simulations, the difference is about 4.28 N for the maximum force and 3.56 N for the minimum force.

It is to say that these analyses can be used to identify the optimal position of the pull bar from the main axle of the pantograph, in order to find the optimal work area of the pantograph, with small variation of the contact force and with a better contact between the pantograph and the contact line.

7. Conclusions

One of the current collecting problems is to assure a permanent contact between the pantograph and the contact line but without using too high forces. Knowing the relation between the contact force and the high of the skate of the pantograph gives the possibility to estimate the place to attach the resort on the pantograph's bar.

In the cases 1, 2, 5, 6, 9, 10 the resort is attached in a slanting way. In the cases 3, 4, 7, 8, 11, 12 the resort is horizontal attached for every high of the pantograph. To estimate the influence of the resort position related to the oscillation point in the cases 1, 3, 5, 7, 9, 11 the resort is attached above of the oscillation point and in cases 2, 4, 6, 8, 10, 12 it is attached below the oscillation point. Analyzing the 12 cases we can conclude:

- If the resort is attached above of the oscillation point all the coefficient of the trigonometrically functions are the same;
- The contact force variation depends strongly by the position of the resort: if the resort is horizontal (above or below of the oscillation point) the variation curve is the same.
- For the situations when the resort is attached by a crank (above or below of the oscillation point), in the relation of the force it appears a new expression.
- The 9th case offers a low variation of the force, assuring a better power collecting for the vehicle.

It is to mention that the pantograph is droved by a resort, but it could be used any other mechanism, like pneumatic or hydraulic drive system.

8. References

1. Ambrosio J, Pombo J, et al. A computational procedure for the dynamic analysis of the catenary-pantograph interaction in high-speed trains. *Journal of Theoretical and Applied Mechanics, Warsaw.* 2012; 50(3):681-99.
2. Niţucă C, Rachid A, et al. Constructive and experimental aspects regarding the electric power collecting for very high speed train. *Analele Univ. Din Craiova.* 2007; 31(II):290-93.

3. Qin Y, Zhang Y, et al. An analysis method for correlation between catenary irregularities and pantograph–catenary contact force. *J. Cent. South Univ*. 2014; 21:3353-60.
4. Eppinger SD, O'Connor DN, Seering WP, Wormley DN. Modeling and experimental evaluation of asymmetric pantograph dynamics. *Transactions of the ASME*. 1988; 110:168-74.
5. Eom BG, Mok JY, Lee HS. Influencing Factors on Dynamic Characteristics of Pantograph of Korean High Speed Train. *IJR Int. Journal of Railway.* 2009; 2(4):187-92.
6. Rachid A. Pantograph Catenary Control and Observation using the LMI Approach. In: *50th IEEE Conference on Decision and Control and European Control Conference (CDC-ECC)* Orlando, FL, USA, 2011, p.2287-92.
7. Lee JH, Kim YG, et al. Performance evaluation and design optimization using differential evolutionary algorithm of the pantograph for the high speed train. *Journal of Mechanical Science and Technology.* 2012; 26(10):3253-60.
8. Huan RH, Zhu W, et al. Vertical dynamics of a pantograph carbon-strip suspension under stochastic contact-force excitation. *Nonlinear Dyn*. 2014; 76:765-76.
9. Pombo J, Ambrósio J. Influence of pantograph suspension characteristics on the contact quality with the catenary for high speed trains. *Computers and Structures*. 2012; 110-111:32-42.
10. Allotta B, Pugi P, Bartolini F. An active suspension system for railway pantographs: the T2006 prototype. *J. Rail and Rapid Transit. Part F.* 2009; 223:15-29.
11. Plesca A. Electric arc power collection system for electric traction vehicles. *International Journal of Electrical Power & Energy Systems*. 2014; 57: 212-21.
12. Satyanarayana Murthy YVV, Sastry GRK, Satyanaryana MRS. Experimental Investigation of Performance and Emissions on Low Speed Diesel Engine with Dual Injection of Solar Generated Steam and Pongamia Methyl Ester. *Indian Journal of Science and Technology*. 2011 Jan; 4(1):29-33.
13. Nituca C. Probleme de captare a curentului de la linia de contact pentru vehicule acţionate electric (in Romanian), Doctoral thesis, Technical University of Iasi, Romania, 2003.

Appendix 1

Nomenclature

A - Distance between the jointed point O1 and the jointed point of the resort, O4.

a, b, c – Constant parameters of the resort;

F – Vertical force due to the resort of the pantograph;

F_r – Force due to the resort;

F_{r0} , F_{rv} – Horizontal and vertical components forces for the force F_r;

G – Weight of the inferior arm of the pantograph;

g – Mass of the pull bar when the resort is not attached directly to the inferior arm;

h_l – High of the skate;

k_0 – Elastic constant of the resort;

k_l = a + b+ c - Elongation of the resort;

x – Variable parameter of the resort;

l – Length of the inferior arm of the pantograph;

M_g – Torque due to the weight of the inferior arm of the pantograph;

M_r – Torque due to the resort;

M_R - the resultant torque;
r – Length of the pull bar.